Development of Ciprofloxacin-loaded Electrospun Fibre Yarns of Application Interest as Antimicrobial Surgical Suture Materials

Jorge Teno , Maria Pardo-Figuerez , Zoran Evtoski , Cristina Prieto , Luís Cabedo , José M. Lagaron *

Posted Date: 9 January 2024

doi: 10.20944/preprints202401.0695.v1

Keywords: PHBVs, electrospinning, fibre yarn, antimicrobial activity

Article

Development of Ciprofloxacin-Loaded Electrospun Fibre Yarns of Application Interest as Antimicrobial Surgical Suture Materials

Jorge Teno [1,*,†], María Pardo-Figuerez [2,†], Zoran Evtovski [2], Cristina Prieto [2], Luis Cabedo [3] and J.M. Lagaron [2,*]

[1] R&D Department, Bioinicia S.L., 46980 Paterna, Spain
[2] Novel Materials and Nanotechnology Group, Institute of Agrochemistry and Food Technology (IATA), Spanish Council for Scientific Research (CSIC), Paterna, Spain
[3] Polymers and Advanced Materials Group (PIMA), School of Technology and Experimental Sciences, Universitat Jaume I (UJI), Castellón, Spain; lcabedo@uji.es
* Correspondence: authors: lagaron@iata.csic.es (J.M. Lagaron), jteno@bioinicia.com (J. Teno)
† These authors contributed equally to this work.

Abstract: Surgical site infections (SSI) occur very frequently during post-operatory procedures and are often treated with oral antibiotics, which may cause some side-effects. This type of infections could be avoided by encapsulating antimicrobial/anti-inflammatory drugs within the surgical suture materials so that these can more efficiently act on the site of action during wound closure, avoiding post-operatory bacterial infection and spreading. This work was aimed at developing novel electrospun biobased anti-infective fiber-based yarns as novel suture materials for preventing surgical site infections. For this, yarns based on flying intertwined nanofibers were fabricated *in-situ* during the electrospinning process using a specially designed yarn collector. The electrospun yarn sutures were made of poly(3-hydroxybutyrate-co-3-hydroxyvalerate) with different contents of 3HV units and contained ciprofloxacin hydrochloride (CPX) as the antimicrobial active pharmaceutical ingredient (API). The yarns were then analyzed by scanning electron microscopy, Fourier transform infrared spectroscopy, wide-angle X-ray scattering, differential scanning calorimetry and *in vitro* drug release. The yarns were also analyzed in terms of antimicrobial and mechanical properties. The material characterization indicated that the varying polymer molecular architecture affected the attained polymer crystallinity, which was correlated with the different drug-eluting profiles. Moreover, the materials exhibited the inherent stiff behavior of PHBV, which was further enhanced by the API. Lastly, all the yarn sutures presented antimicrobial properties for a time release of 5 days against both gram positive and gram-negative pathogenic bacteria. The results presented highlight the potential of the herein developed antimicrobial electrospun fiber yarns as potential innovative suture materials to prevent surgical infections.

Keywords: PHBVs; electrospinning; fibre yarn; antimicrobial activity

1. Introduction

Sutures are a key component in every surgical procedure that requires bringing together damaged tissues, promote healing after an injury, ligation of blood vessels, hemostasis, among others [1–3]. The materials used in sutures and its manufacturing process have improved over the years, generating multiple suture options depending on the site of action, depth, tension, type of material and mechanical strength [3]. However, little has been pursued on enhancing their therapeutic effect to treat wounds locally to avoid surgical site infections (SSI) [4]. SSI occurs quite often post-operatory and are normally treated with oral antibiotics prior and post-surgery, which may lead to unnecessary side-effects. Additionally, if oral therapy fails, the infection can spread and microorganisms can grow on the sutures, hindering the wound healing process whilst migrating and infecting adjacent tissues [5,6]. Thus, it is necessary to incorporate antimicrobial/ anti-inflammatory drugs to the sutures to create high local drug concentrations without excessive systemic levels to efficiently act on the site of action [7].

 doi:10.20944/preprints202401.0695.v1

The incorporation of antimicrobial drugs into the sutures has been frequently achieved using melt spinning [8], dip coating [9], layer by layer [6] or soaking procedures, among others [9,10]. A study reported by Wang et al. [11] used a commercial silk fibre previously coated with sequential layers of poly(allylamine hydrochloride), dextran and hyaloplasm acid. Thereafter, these were soaked into an aqueous solution of ibuprofen to obtain the final drug eluting material. The release studies showed that up to 76% of the loaded ibuprofen was released in 24 h [11]. Although effective, these types of techniques do not appropriately encapsulate the component of interest and consequently controlling their release kinetics and their stability over time can become a challenge.

Electrospinning has been used to produce nano and microfibrous structures that can efficiently incorporate drugs within the polymeric matrix in a single step [1,12,13]. This technique is based on the use of voltage into a polymeric solution that enables the formation of electrospun fibres, which are deposited into a collector [14]. The versatility of the technique allows depositing the materials in a wide range of collector geometries, leading to the generation of planar materials such as mats, or 3D-like structures such as conduits [15] or yarns [16]. Regarding the latter, a modification on the collector set up can generate a continuous thread-like structure made of nano and microfibres that may mimic the structure of a yarn [16]. This type of material presents many advantages when compared to other yarn manufacturing processes [1] and may be key to replace the traditional threads in terms of properties and functional performance. For instance, electrospun fibres can encapsulate active components within their structure, providing a localized, controlled and reliable drug delivery if we compared to other drug eluting manufacturing processes, such as soaking or dip coating procedures. Additionally, electrospinning does not require high processing temperatures, and so the technique could generate sutures that encapsulate thermolabile APIs such as proteins, peptides growth factors, DNA, or other sensitive pharmaceutical compounds that would not be feasible when using melt spinning. The use of electrospinning has been recently used to generate sutures, proving its potential for this application. As an example, Kashiwabuchi et al. [17] developed and manufactured electrospun sutures composed of poly(L-lactide), polyethylene glycol (PEG) and levofloxacin for ophthalmic surgery. The authors achieved a sustained release of the antibiotic for months as well as a strong bacterial zone inhibition of S. epidermidis after 7 days in release media. PLLA is one of the gold standard biopolymer used for biomedical applications, however, other biopolymers such as polylactide glycolide (PLGA) [18], polydioxanone (PDS) [19] polylactide (PLA) [6,20] or polyhydroxyalkanoates (PHAs) [20,21] can also be used as innovative materials to generate sutures.

PHAs are a family of biodegradable and highly biocompatible materials that have already proven success in biomedical applications [22]. Although plenty of PHAs have been discovered, the most commonly investigated are poly(3-hydroxybutyrate) (PHB) and its copolymer poly(3-hydroxybutyrate-co-3-hydroxyvalerate) (PHBV). PHB has a high crystallinity and macromolecular organization, resulting in a stiff and brittle material that lacks of mechanical strength [23]. On the contrary, the co-polyester PHBV shows improved thermal and mechanical properties, which varie with the content of 3HV units present in the polyester. In fact, a higher content in 3HV implies a lower crystallinity and a broader thermal processing, resulting in a more flexible, ductile, and tough material to work with [referencia]. Hence, PHBV has become an attractive candidate for biomedical applications [23,24]. Currently, commercial PHBV is limited to 3HV contents of 2 mol%, which present similar properties to those of commercial PHB grades. For this reason, new materials with different 3HV units are being synthesized and investigated to achieve a better balance in properties for numerous applications [23].

The present study was aimed at the development of antibiotic drug eluting PHBV yarns prepared by electrospinning with a custom designed funnel collector, to prevent SSI. For this, PHBVs with different 3HV contents (2, 10 and 20 mol%) and ciprofloxacin hydrochloride (CPX) were selected as the material and drug antimicrobial model for the yarn developments, respectively. CPX is an antibiotic belonging to the family of fluoroquinolones, with a broad antibacterial activity against Gram-negative and Gram-positive bacteria [25]. The studies performed on the electrospun yarns included microscopical, thermal and mechanical characterization to unveil the surface morphology,

 doi:10.20944/preprints202401.0695.v1

physical and mechanical features of the materials. To determine the suitability of the material as drug eluting materials, in vitro release studies of CPX and antimicrobial properties were carried out for the different CPX-PHBVs manufactured.

2. Materials and Methods

2.1. Materials

Ciprofloxacin hydrochloride (CPX) was obtained from Uquifa (Castellbisbal, Spain). The PHBV2 (ENMAT Y1000P), was purchased from Tianan Biologic Materials (Ningbo, China) and delivered in the form of pellets. According to the manufacturer, the 3HV fraction in the commercial copolyester is 2 mol%. The polyester PHBV10 with a percentage of 10 mol% of 3HV content was kindly provided by Venvirotech SL (Santa Perpètua de Mogoda, Spain), and the PHBV20 with 20 mol% of 3HV was produced at Universida de NOVA de Lisboa (Lisbon, Portugal) using mixed microbial cultures (MMCs) as detailed in previous works [26]. The solvent 2,2,2-trifluoroethanol (TFE, ≥99%) was purchased from Alfa Aesar™ (Karlsruhe, Germany). All the polymers and reagents were used as received without further purification.

2.2. Electrospun Fibre Yarn

Prior to yarn production, different PHBVs solutions were prepared by dissolving each biopolymer at 8 wt.% in TFE. The CPX was added at 20 wt.% in relation to the polymer. Solutions were prepared by adding the corresponding amount of polymer and CPX in the solvent under stirring overnight at 37 °C. All polymer solutions were processed in a Fluidnatek® LE-500 pilot-plant tool manufactured by Bioinicia S.L. (Valencia, Spain) adapted with a specifically engineered fibre yarn accessory (See Figure 1 for the schematics of the equipment and Supplementary Material for a video of the set-up running). The spinning solution was passed through a multi-needle system by means of an injection pump. The polymer was exerted into both sides of the yarn and formed fibres under the action of a high voltage electric field. The orientated fibres formed in the air and were directed by the force of the rotating funnel, which ultimately twisted the oriented fibres to form fibre yarns. The first thread of the fibre yarn was placed in a yarn collector at the other side of the equipment. The conditions for yarn production were set as described in Table 1. Each solution was electrospun for under a controlled environment with 30°C and 30% RH. The collected sutures were maintained at room temperature in a desiccator at 0% RH until further analysis.

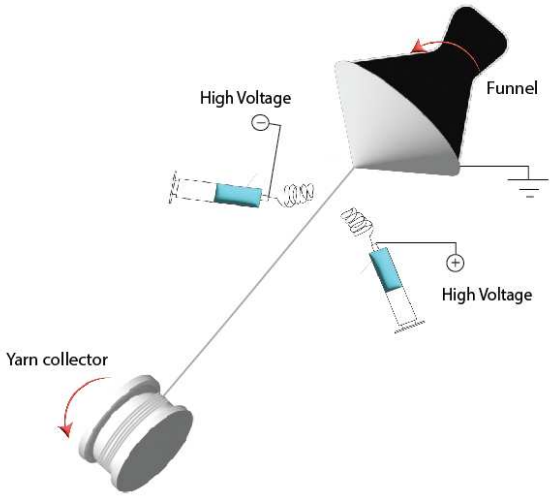

Figure 1. Schematics of the fibre yarn set up.

Preprints (www.preprints.org) | NOT PEER-REVIEWED | Posted: 9 January 2024 doi:10.20944/preprints202401.0695.v1

Table 1. Optimal electrospinning parameters for the different solutions tested.

Sample ID	Flow-rate (mL/h)	Voltage V+/V- (kV)	Funnel to yarn collector distance (cm)	Needle distance to funnel (cm)	Funnel speed (rpm)	Yarn collector (rpm)
PHBV2 PLACEBO	12	10/-10	26.5	34	300	5
PHBV2 + CPX	10	13/-13	26.5	35.5	300	5
PHBV10 PLACEBO	5	18/-18	25.5	34	300	5
PHBV10 + CPX	5	18/-18	28.5	34	300	5
PHBV20 PLACEBO	3	15/-15	24.5	34	300	5
PHBV20 + CPX	5	15/-15	26.5	35.5	300	5

2.3. Yarn Characterization

2.3.1. Morphology

The PHBV electrospun fibre yarns with and without CPX were examined by scanning electron microscopy (SEM) using a Phenom XL G2 Desktop microscope (Thermo Fisher Scientific, Waltham, MA, USA) with an electron beam acceleration of 5 kV. Samples were previously sputtered with a gold-palladium mixture for 3 min under vacuum. Average fibre diameter based on at least 100 fibres was determined using a Phenom ProSuite Software on SEM images.

2.3.2. Wide-Angle X-ray Scattering (WAXS)

Wide-angle X-ray scattering measurements were performed using a Bruker AXS D4 Endeavor diffractometer. The samples were scanned at room temperature in reflection mode using incident Cu K-alpha radiation (Cu Kα = 1.54 Å), while the generator was set up at 40 kV and 40 mA. The data were collected over a range of scattering angles (2Θ) in the 5–40° range.

2.3.3. Attenuated Total Reflection - Fourier Transform Infrared Spectroscopy (ATR-FTIR)

The presence of the CPX in the polymer matrix was evaluated by Fourier transformed infrared spectroscopy and measured with a Bruker Tensor 37 FT-IR Spectrometer (Bruker, Ettlingen, Germany) coupled with the ATR sampling accessory Golden Gate (Specac Ltd., Orpington, UK). Spectra were collected from the average of 64 scans in the range of 4000-600 cm-1, with a resolution of 4 cm^{-1}.

2.3.4. Thermal Analysis

The electrospun fibre yarns were studied by differential scanning calorimetry (DSC) using a DSC-8000 analyzer from PerkinElmer, Inc. (Waltham, MA, USA), equipped with a cooling accessory Intracooler 2 also from PerkinElmer, Inc. Approximately 3 mg of each sample were placed in standard aluminum pans and heated from 25 to 250°C at a rate of 10 °C/min using a nitrogen flow of 20 mL/min as the sweeping gas.

2.3.5. Mechanical Tests

The mechanical properties were determined using an universal testing machine (Shimadzu AGS-X 500 N) at room temperature with a cross-head speed of 10 mm/min and an initial distance

Preprints (www.preprints.org) | NOT PEER-REVIEWED | Posted: 9 January 2024 doi:10.20944/preprints202401.0695.v1

between clamps (L_0) of 25 mm. The method was based in ASTM D638 standard. Tensile modulus (E), tensile strength (σ_b) and elongation at break (ε_b) were calculated from the stress–strain curves. Yarns specimens ($n \geq 5$) of 40 mm in length were tested.

2.3.6. In Vitro Drug Release, Kinetics Study

Drug release was evaluated using an UV-spectrophotometer DINKO UV4000 (Barcelona, Spain). The release of CPX-loaded yarns (0.5 mg approx.) into an aqueous phosphate buffer solution (pH 7.4) medium was monitored by measuring the absorbance at 270 nm at predetermined times whilst stirring at 100 rpm at 37 °C. All the experiments were carried out in triplicate and the cumulative release rate was reported as mean ± S.D.

To determine the experimental loading of CPX within the fibre yarns, ca. 3 mg of CPX-loaded yarns were dissolved in 60 mL of TFE to fully dissolve both CPX and polymers. The resulting solution was stirred at 100 rpm for an hour at 37 °C, and then analyzed by UV-spectrophotometer DINKO UV4000 (Barcelona, Spain). The reading was compared against a calibration curve produced using standard samples of 1–8 µg/mL of CPX in HFIP. The absorbances at 270 nm were recorded and the experimental CPX loading (%) in the fibres was calculated using the following equation:

$$CPX\ Loading\ (\%) = \frac{m_d}{m_p} \times 100 \quad (1)$$

where m_d is the mass of the drug obtained experimentally as described above, and m_p is the total mass of the sample analyzed.

Additionally, the semi-empirical mathematical model of Korsmeyer-Peppas was applied to study the kinetics of drug release from the yarns. The dosage form can be represented as follows:

$$Q = kt^n \quad (2)$$

where Q is the amount of drug released in time t, K is the Korsmeyer-Peppas release rate constant and n is release exponent, which depends on the type of drug polydispersity, geometry, and transport. Depending on the release exponent, diffusional release mechanisms were classified as; $n<0.5$ pseudo-Fickian diffusional behavior, $n = 0.5$ Fickian diffusion, $0.5<n<1$ non-Fickian diffusion, $n = 1$ case II transport (zero order release), and $n>1$ super case II transport [27].

2.3.7. Antimicrobial Activity

Staphylococcus aureus (*S. aureus*) CECT240 (ATCC 6538p) and Escherichia coli (*E. coli*) CECT434 (ATCC 25922) strains were obtained from the Spanish Type Culture Collection (CECT, Valencia, Spain). The bacteria were thawed at 37 °C under agitation at 180 rpm for 24 h and were then diluted in a 1:1000 proportion in a Mueller-Hinton broth until obtaining a concentration of $3–5\times10^5$ colony-forming unit (CFU)/mL [28].

The antimicrobial activity of the fibrous yarns was studied by the disc diffusion method, following the protocols by Clinical and Laboratory Standards Institute (CLSI) with some modifications [28,29]. Yarns of approximately 1 cm length with and without CPX were deposited onto the Mueller-Hinton solid agar surface previously inoculated with 100 µL of *S. aureus and E. coli* ($3–5 \times 10^5$ CFU/mL). The samples were analyzed in triplicate and incubated at 37 °C for 5 days hours. Inhibition diameters were measured after 1, 3 and 5 days, and the results are given as the mean ± S.D.

2.3.8. Statistical Analysis

To detect differences among the fibre and yarn diameter, an unpaired t test was used using a GraphPad Prism 8.0.1 software. Differences were considered statistically significant (*) when $p \leq 0.05$.

Preprints (www.preprints.org) | NOT PEER-REVIEWED | Posted: 9 January 2024 doi:10.20944/preprints202401.0695.v1

3. Results

3.1. Morphological Characterization of Yarn Sutures

Upon yarn processing, different behaviors were observed among the different PHBVs. The PHBV with a higher valerate content (PHBV20) caused continuous breaking during initial yarn formation, whereas PHBV with lower 3HV content, led to a more stable process and little optimization was needed to collect meters of yarn, as it was optimally the case of PHBV2. At optimal processing conditions, the latter material could be processed at lower voltage and higher flow rates, suggesting better spinnability than their higher 3HV content counterparts.

The produced yarns were characterized by SEM to analyze the morphology of the fibres, as well as the overall diameter of the yarns. In terms of fibre diameter, the neat PHBV2, PHBV10 and PHBV20 and their counterparts containing CPX had a fibre diameter within the micrometer range (see Figure 2), with a preferential fibre orientation along the yarn collection. The presence of CPX in the yarns reduced the fibre diameter slightly when compared to the neat PHBV yarns, although the results were not statistically significant for any of the samples ($p>0.05$).

The overall diameter of PHBV2, PHBV10 and PHBV20 yarns was ≈300-500 µm, as gathered in Figure 2, being the PHBV2 yarn thicker. In this case, the addition of CPX resulted in a reduction in the overall yarn diameter, which was statistically significant for all three PHBVs analyzed. This phenomenon could be associated with an accumulative effect of the slightly fibre size reduction discussed previously.

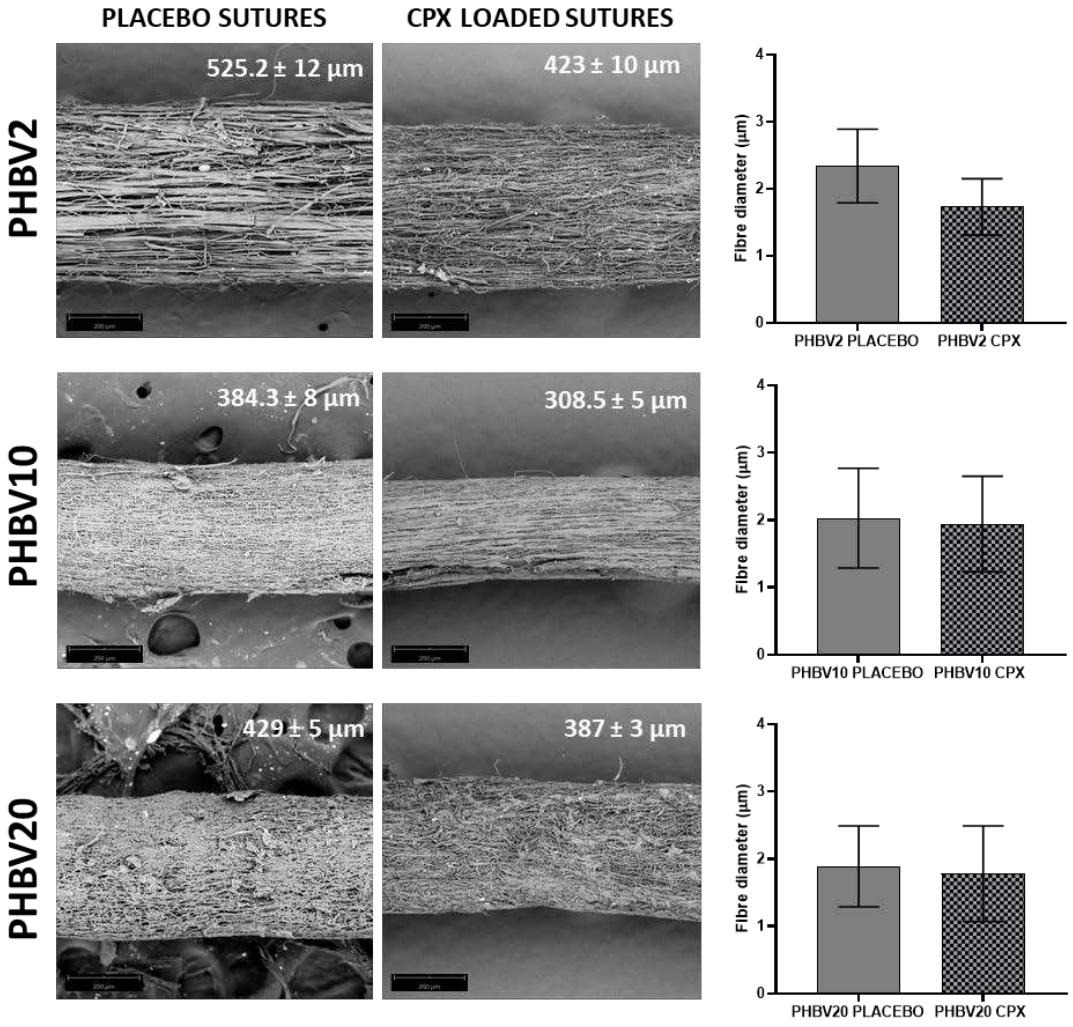

Figure 2. Scanning electron microscopy (SEM) micrographs of the fibre placebo PHBV yarns at 2% (PHBV2), 10% (PHBV10) and 20% HV content (PHBV20) and the CPX-PHBV loaded yarns. Values in

Preprints (www.preprints.org) | NOT PEER-REVIEWED | Posted: 9 January 2024 doi:10.20944/preprints202401.0695.v1

the images represent the average yarn diameter size ± S.D. On the right, graphs illustrate the fiber diameter of PHBV2, PHBV10 and PHBV20 with and without CPX. The scale bars are of 200 μm in all micrographs.

3.2. Thermal, Crystallinity and Molecular Characterization

Yarns with and without CPX were analysed to obtain information about the crystallinity of the polymers in the presence of CPX. Figure 3 shows the DSC thermograms of the PHBV and PHBV-CPX yarns and pure CPX. The thermogram of the pure CPX (black line present in Figure 3a, b and c) showed, in the range screened, a broad diffuse endothermic peak around 150°C, which was attributed to dehydration, in agreement with previous studies [30–33]. The melting point of the API occurs in the range of 255-257 °C. The thermograms of the placebo PHBV2 and PHBV10 showed an endothermic peak associated with the melting point of the crystalline phase at 173 °C and 174 °C, respectively. The two polymers showed an enthalpy of fusion of 90.9 J/g and of 70.5 J/g, respectively, suggesting the expected higher crystallinity of the PHBV2 [23]. From observation of Figure 3, the PHBV2-CPX and PHBV10-CPX yarns showed a decrease in both melting point, 161.1°C and 161.8°C, and enthalpy of fusion, 71.8 J/g and 61.8 J/g, than the neat biopolymer yarns, suggesting a decrease in polymer crystallinity and crystal size and/or density induced by the presence of the API. The thermograms of PHBV20 and PHBV20-CPX, presented a weaker and broader melting behavior, with maximums of melting at 154.4 °C and 156.7°C and enthalpies of fusion of 66.2 J/g and 50.21 J/g, respectively. The enthalpies of fusion of the drug loaded samples included the small contribution of the shoulder at the lower temperature side of the melting peak, which might be associated to the CPX dehydration, hence even overestimating to some extent their crystallinity. As expected, the melting temperatures and enthalpies decreased with an increase in the 3HV content in the copolymers, ascribed to a decrease in crystallinity and crystal perfection [24][34,35]. Additionally, the PHBV-CPX peaks are usually broader and smaller than those of the neat PHBV yarns, which may also be attributed to the formation of crystals with lower perfection and broader size distribution, suggesting an overall deterioration of the crystalline morphology for the PHBV-CPX materials [35,36].

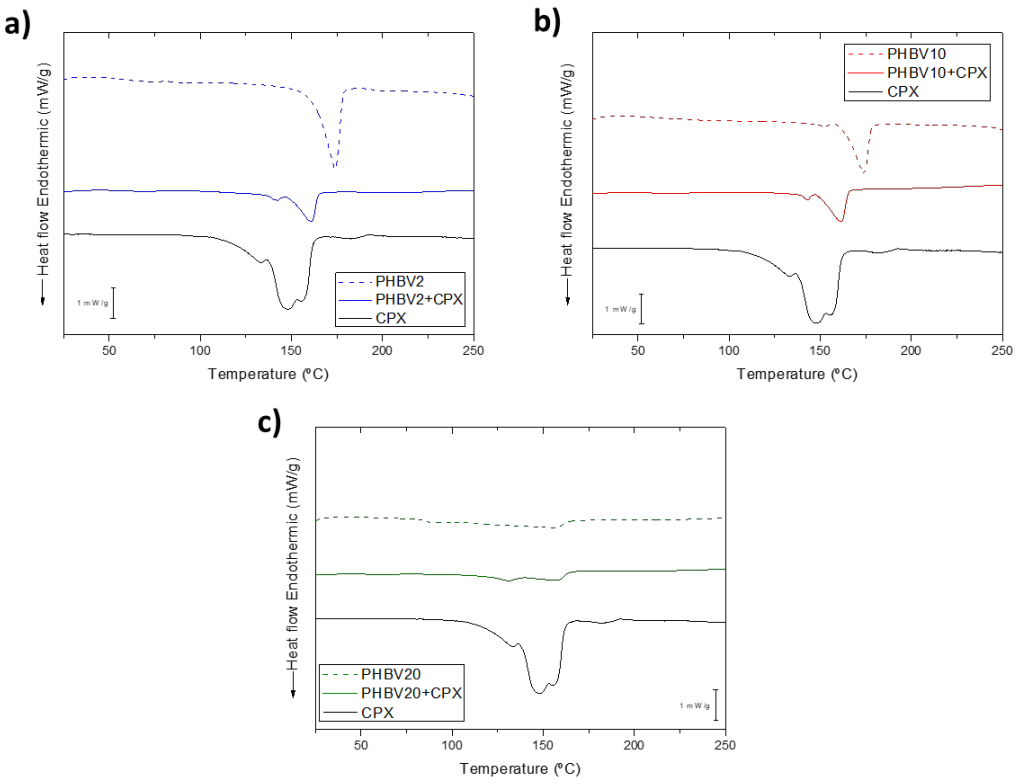

Figure 3. a) DSC thermograms of PHBV2 placebo, PHBV2+CPX and *pure CPX*. b) PHBV10 placebo, PHBV10+CPX and *pure CPX*. c) PHBV20 placebo, PHBV20+CPX and *pure CPX* fibre yarns samples.

 doi:10.20944/preprints202401.0695.v1

To assess further the crystalline morphology of the polymers but also of the drug in the fibers the samples were analyzed by WAXS (Figure 4a). The pure CPX, exhibited the expected X-ray diffraction pattern of a crystalline material with three main sharp peaks at around 2θ at 8.2°, 9.0° and 26.5°, in agreement with previous studies [32]. The X-ray patterns of PHBV with and without CPX showed the typical main peaks at 2θ of 13.7°, 17.0°, 25.0° and 27.0° corresponding to the (020), (110), (121) and (040) lattice planes of the orthorhombic unit cells of PHBV, being these sharper for the lowest HV content sample, which suggests a more robust crystalline phase for the PHBV2 in agreement with previous studies [23,37,38]. The crystalline peaks seen in the CPX spectra were not identified in the PHBV yarns with CPX; however, a distinct new peak at 6.4° arose in the spectra of all the CPX loaded yarns, which was not present in the spectra of pure CPX. The appearance of this new peak might be related to the development of new ordered forms in the blend due to potentially strong interactions among polymer and drug [39].

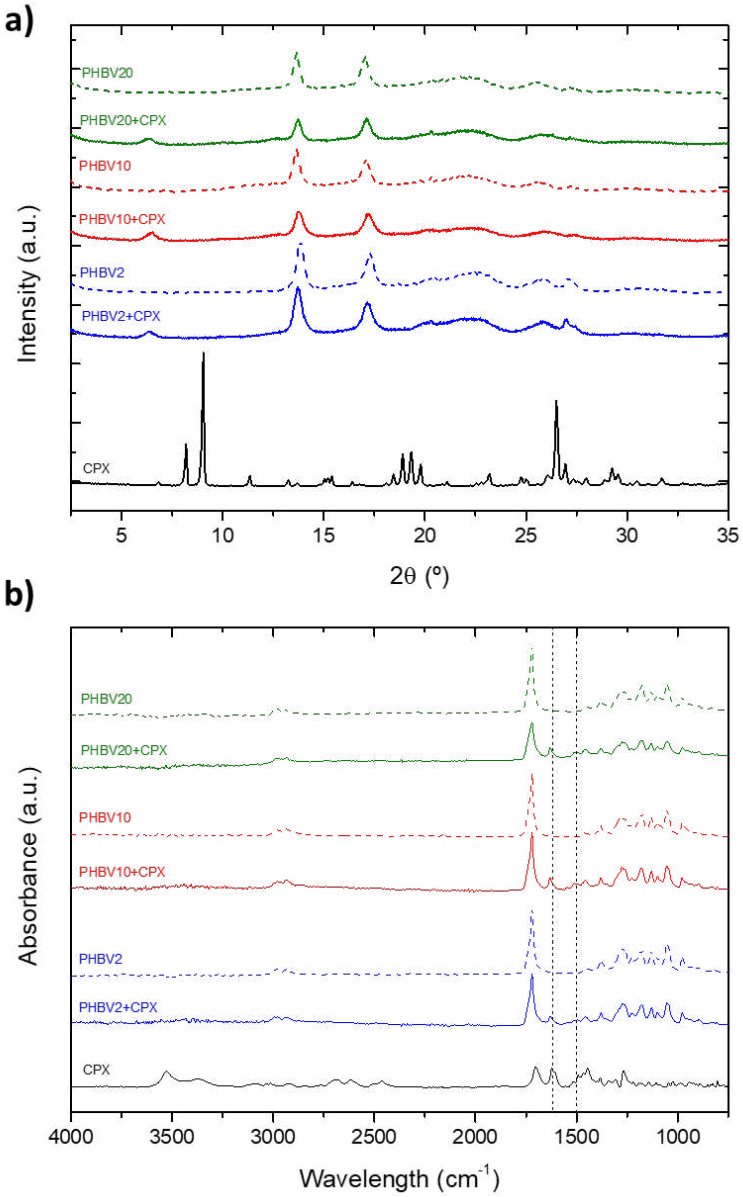

Figure 4. a) WAXS spectra and b) ATR-FTIR spectra of fibre yarns samples of *pure CPX* (black line), placebo electrospun yarns (dash lines) and CPX loaded yarns. The dashed straight lines indicate the CPX characteristic peaks at 1622 and 1492 cm^{-1}.

Preprints (www.preprints.org) | NOT PEER-REVIEWED | Posted: 9 January 2024 doi:10.20944/preprints202401.0695.v1

Figure 4b shows a comparison of the ATR-FTIR spectra for pure CPX, neat PHBV and CPX-loaded PHBV yarns. The yarns of PHBVs showed their characteristic bands at 1718 cm^{-1}, which is related to C=O stretching vibrations. The CH_3 asymmetric and symmetric deformation was observed at 1452 cm^{-1} and 1379 cm^{-1}, respectively, whilst C–O–C stretching was observed at 1278 cm^{-1}, 1224 cm^{-1}, and 1178 cm^{-1}, in agreement with other studies [40]. Regarding the CPX loaded PHBV yarns, two non-overlapping characteristic peaks of the drug where found at 1622 and 1492 cm^{-1} (dashed straight lines in the Figure 4a), associated with C=O and C-H stretching, respectively [41,42], thus confirming the presence of the drug in the yarns. As no spectroscopic alterations or new features ascribed to degradation or reaction of the API with the polymer were unambiguously detected, the polymer-API blends were considered stable.

3.3. Process Loading Efficiency and In Vitro Release

Table 2 gathers the results of the measured percentage of CPX loading found in the different electrospun yarns with regard to the drug put in solution prior to electrospinning. The data suggest that the process efficiency is very high, since more than 95% of the drug in solutions is encapsulated in the yarns.

Table 2. Process CPX loading efficiency (%) measured in the different electrospun yarns.

Sample ID	CPX loading in the yarns (%)
PHBV2+CPX	97.33±2.42
PHBV10+CPX	95.50±7.50
PHBV20+CPX	96.54±4.43

Figure 5 illustrates the cumulative drug-elution from the yarns. The release curves were fitted to a Korsmeyer-Peppas model (Table 4). For all the samples, the values of the regression coefficient (r^2) were high for the model, indicating a good fitting and also suggesting that more than one type of drug release mechanism is taking place. In fact, the corresponding n values of the evaluated samples were all below 0.5, indicating that the drug release seemed to follow a pseudo-Fickian diffusional behavior.

Table 4. Model parameters of CPX release profiles obtained from Korsmeyer-Peppas model.

Korsmeyer-Peppas			
Sample ID	K	n	r^2
PHBV2+CPX	28.88	0.12	0.99
PHBV10+CPX	17.68	0.25	0.99
PHBV20+CPX	52.56	0.15	0.99

From a phenomenological view-point the yarns made of PHBV2 exhibited a burst released followed by an arrested one after ca. 24 h, achieving a value of ca. 50% after 95 hours. The initial burst release could be related to the presence of CPX on and near the fibre surface and can be quantitatively described by the parameter K (Korsmeyer-Peppas release rate) gathered in Table 4. The arrested release after 24 hours is likely attributed to drug more tightly bound inside the fibers and requiring a more tortuous path to diffuse out, since the PHBV crystals are thought to arrest the CPX elution.

For the PHBV yarn containing 10 mol% 3HV, a somewhat lower initial burst release was observed, followed by a somewhat faster sustained release reaching near 60% after 95 hours. This initial burst behaviour is quantitatively characterized by the parameter K (Korsmeyer-Peppas release rate), since it presents the lowest value in comparison with the other two yarns. As the crystallinity of the PHBV2 sample was found to be higher than this of the PHBV10, the initially higher burst release could be associated to the forming crystals of the PHBV2 sample pushing out more of the drug towards the outside the fiber.

Preprints (www.preprints.org) | NOT PEER-REVIEWED | Posted: 9 January 2024 doi:10.20944/preprints202401.0695.v1

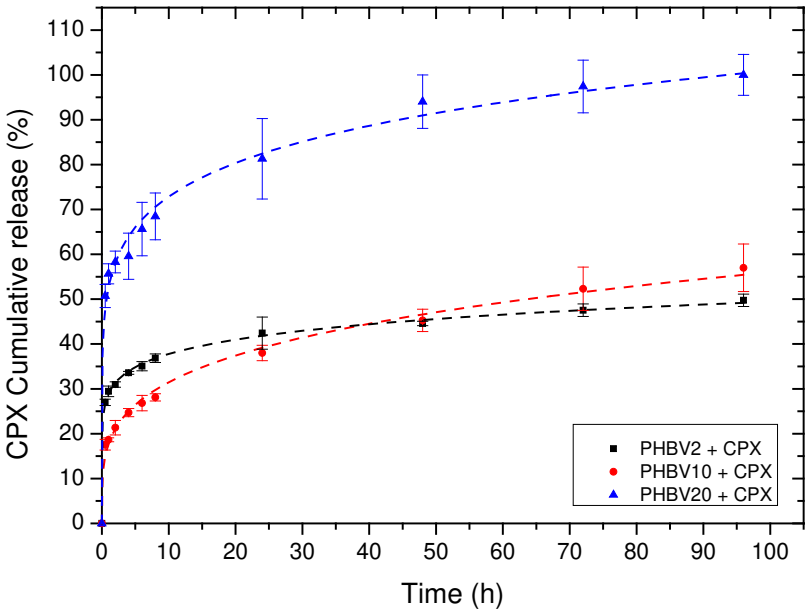

Figure 5. Drug release data comparing the different yarns containing CPX. Dashed lines are the Korsmeyer-Peppas fitting. Values are presented as the mean ± SD (n=3).

The yarn with the highest amount of 3HV units (20% mol), presented a burst release of approx. 70% after 10 h, followed by an arrested release up to ca. 100% after 95 hours. Such differing behaviour could be due to the clearly more ill-defined crystalline phase suggested by the DSC and WAXS analysis, hence facilitating a faster drug elution.

3.4. Antimicrobial Activity

Figure 6 represents the inhibition zones of the prepared yarns with and without CPX for both the Gram-positive and Gram-negative bacteria for up to 5 days. The yarns without CPX (PHBV2, PHBV10 and PHBV20) showed no inhibition zone for *S. aureus* and *E. coli*, indicating limited antibacterial effects. In the case of the CPX-loaded materials (PHBV2+CPX, PHBV10+CPX and PHBV20+CPX), very large inhibition zones were observed. An inhibition zone larger than 1 mm indicates a somehow strong antibacterial effect at the site of action [6,43]. In the case of PHBV2+CPX, the halo size was larger than 30 mm for both strains from day 1 to day 5, with a slightly reduction towards the end of the experiment. PHBV10+CPX and PHBV20+CPX showed a similar trend, with halo sizes larger than 30 mm in all cases, especially for PHBV10+CPX for the strain *E. coli.*

The effectiveness of loaded CPX materials as antimicrobial agents has been reported in the literature. For instance, in a study reported by our research group, patches made of blends of polyesters loaded with CPX reported an inhibition zone of approx. 5 cm after 24 hours, proving that CPX-loaded fibres could efficiently act as antimicrobial multilayer systems [44]. Another study by Liu *et al.* reported the incorporation, characterization and drug release of CPX in sutures by dip-padding, but no data was presented for *in vitro* antimicrobial testing [45]. Alternatively, the sutures loaded with a fluoroquinolone family compound (levofloxacin), showed that 4% of loaded PEG/PLLA created a 2-cm inhibition zone after 24 hours of drug release. Besides, 7 days after the drug-loaded sutures still provided bacterial inhibition confirming that biologically active antibiotic was being released from the suture in an amount sufficient to eliminate surrounding bacteria [17], similar to what has been observed in this study.

Preprints (www.preprints.org) | NOT PEER-REVIEWED | Posted: 9 January 2024 doi:10.20944/preprints202401.0695.v1

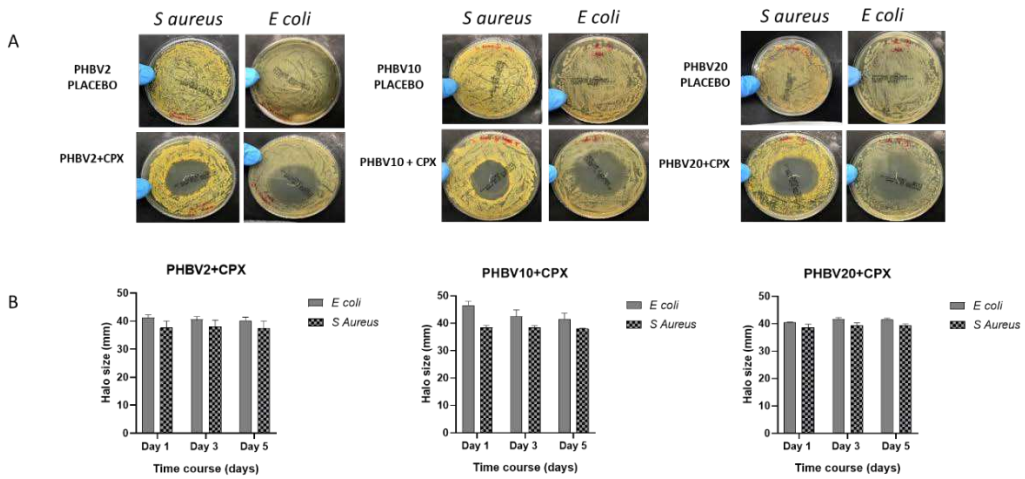

Figure 6. A) Representative photographs of the growth inhibition of PHBV yarns with different HV contents (PHBV2, 10 and 20) with and without CPX against Escherichia coli (E. coli); and Staphylococcus aureus (S. aureus) after 5 days of culture. B) Halo inhibition size of PHBV sutures with different HV contents (PHBV2, 10 and 20) with CPX against Escherichia coli (E. coli); and Staphylococcus aureus (S. aureus) after 1, 3 and 5 days of culture.

3.5. Mechanical Properties

Tensile modulus (E), tensile strength (σ_b) and elongation at break (ε_b) were calculated from the stress–strain curves. Table 5 shows the mechanical properties of the yarns with and without CPX. When looking at the placebos, the tensile modulus tended to decrease with increasing 3HV content. On the overall, the three materials exhibited a brittle behavior. The incorporation of CPX into the PHBV yarns tended to increase the tensile modulus and also the tensile strength. This increase in yarn rigidity may indicate that the CPX acts as a reinforcing filler for the polymer matrix. Interestingly, other studies using electrospun drug eluting sutures, more specifically anesthesia, reported that the suture's strength decreased as the concentration of the drug in the suture increased. In this particular study, the loading of the drug in the suture varied from 5-22% [4]. In the present study, the use of ciprofloxacin at 20% loading seemed to stiffen the yarns. In another study conducted by Kamal et al. [46], planar electrospun PHBV containing cephalexin increased the elastic modulus and the tensile strength [46]. In another study, PLLA yarns showed a higher tensile stress when compared to PLLA yarns loaded with curcumin [47]. The differences in mechanical properties among the studies can be influenced by many factors such as the type of drug used, its dispersion throughout the polymeric matrix, crystallinity and hardness of the drug, interactions between the drug and the polymer, as well as the yarn morphology [1].

Table 5. Mechanical properties of ciprofloxacin loaded PHBV sutures.

Sample	E (MPa)	σ_b (MPa)	ε_b (%)
PHBV2	660 ± 131	8.4 ± 1.8	14.3 ± 1.6
PHBV2+CPX	996 ± 224	14.5 ± 3.2	11.0 ±0.5
PHBV10	575± 281	10.1± 2.6	14.8 ± 5.1
PHBV10+CPX	1099 ± 204	13.6 ± 2.0	14.7 ± 9.1
PHBV20	438 ± 126	8.5 ± 2.4	10.6 ± 3.2
PHBV20+CPX	731 ± 334	11.1 ± 1.8	16.5 ± 6.3

When comparing our materials to commercially available sutures, it is noteworthy mentioning that these proof-of-concept yarns still need further development when it comes to mechanical properties. Although the herein presented electrospun yarns allowed optimum drug release, antimicrobial properties and showed enhanced strength when the antibiotic was incorporated, these are still not as robust as current commercially available sutures. For example, MonoMax® sutures,

which are commercial sutures made of poly-4-hydroxybutyrate, reported a young modulus of 485 MPa [48], which is lower than the PHBV-CPX yarns reported here. However, the elongation at break is much higher than the herein developed yarns [48–50].

On the other hand, when analyzing studies based on drug eluting sutures made by electrospinning, the literature also reports mechanical properties below the cited comparable commercial standards [3,4,17]. Further studies will involve the use of polymer blends [51] and core-sheath strategies [52] to balance the mechanical properties.

4. Conclusions

This study has shown for the first time the development and manufacture of electrospun drug eluting yarns made of three PHBV polymers with varying 3HV contents loaded with ciprofloxacin hydrochloride. The materials were manufactured by needle-based electrospinning but adapted with a custom designed funnel collector to synthesize in-situ and continuously yarns based on nanofibers. The morphology of the yarns for different PHBV grades showed cylindrical structures of approximately 300-500 μm made of thin fibers with averaged diameters in the range 1-3 μm. The API appeared to be in an amorphous state within the yarns and the polymer crystallinity was found to decrease with increasing the HV content in the copolymers, which was correlated with the release profiles. The antibacterial activity of the different sutures was measured by halo size, suggesting a strong inhibition growth for two typical pathogenic strains after 5 days of culture, thus proving they that can be suitable for post-operation sutures in order to avoid surgical site infections. The yarns developed presented an increased stiffness when CPX was incorporated; however, when comparing the mechanical performance with other existing commercially available suture materials, it is considered that a somewhat higher elasticity could be more optimal for the application. Nevertheless, the materials developed present an interesting biobased and anti-infective alternative to the other conventional materials used today in wound healing and closure applications.

Supplementary Materials: The following supporting information can be downloaded at: www.mdpi.com/xxx/s1, Video S1: Fiber yarn device operating.

Author Contributions: Conceptualization, J.T, M.P.-F. and J.M.L. methodology, J.T., M.P.-F. and J.M.L.; analysis and characterization, M.P.-F., C.P., J.T., Z.E .and L.C.; investigation, J.T. and M.P.-F.; data curation, J.T. and M.P.-F.; writing—original draft preparation, J.T. and M.P.-F.; writing—review and editing, M.P.-F., C.P., J.T. and J.M.L.; funding acquisition, J.M.L.. All authors have read and agreed to the published version of the manuscript.

Funding: This study was supported by the Agencia Valenciana de Innovación (AVI), project INNEST/2022/3-25-64 and by the Spanish Ministry of Science and Innovation (MICIN), projects PID2021-128749OB-C31 and TED2021-130211B-C32.

Institutional Review Board Statement: Not applicable.

Informed Consent Statement: Not applicable.

Data Availability Statement: Not applicable.

Acknowledgments: The authors would like to acknowledge the Polymer Technology joint unit UJI - IATA-CSIC.

Conflicts of Interest: The authors declare no conflict of interest.

References

1. Wu, S.; Dong, T.; Li, Y.; Sun, M.; Qi, Y.; Liu, J.; Kuss, M.A.; Chen, S.; Duan, B. State-of-the-art review of advanced electrospun nanofiber yarn-based textiles for biomedical applications. *Appl. Mater. Today* **2022**, *27*, doi:10.1016/j.apmt.2022.101473.
2. Xu, L.; Liu, Y.; Zhou, W.; Yu, D. Electrospun Medical Sutures for Wound Healing: A Review. *Polymers (Basel).* 2022, *14*.
3. Arora, A.; Aggarwal, G.; Chander, J.; Maman, P.; Nagpal, M. Drug eluting sutures: A recent update. *J. Appl. Pharm. Sci.* **2019**, *9*, 111–123, doi:10.7324/JAPS.2019.90716.
4. Weldon, C.B.; Tsui, J.H.; Shankarappa, S.A.; Nguyen, V.T.; Ma, M.; Anderson, D.G.; Kohane, D.S. Electrospun drug-eluting sutures for local anesthesia. *J. Control. Release* **2012**, *161*, 903–909,

doi:10.1016/j.jconrel.2012.05.021.
5. García-Vargas, M.; González-Chomón, C.; Magariños, B.; Concheiro, A.; Alvarez-Lorenzo, C.; Bucio, E. Acrylic polymer-grafted polypropylene sutures for covalent immobilization or reversible adsorption of vancomycin. *Int. J. Pharm.* **2014**, *461*, 286–295, doi:10.1016/j.ijpharm.2013.11.060.
6. Wang, X.; Liu, P.; Wu, Q.; Zheng, Z.; Xie, M.; Chen, G.; Yu, J.; Wang, X.; Li, G.; Kaplan, D. Sustainable Antibacterial and Anti-Inflammatory Silk Suture with Surface Modification of Combined-Therapy Drugs for Surgical Site Infection. *ACS Appl. Mater. Interfaces* **2022**, *14*, 11177–11191, doi:10.1021/acsami.2c00106.
7. Günday, C.; Anand, S.; Gencer, H.B.; Munafò, S.; Moroni, L.; Fusco, A.; Donnarumma, G.; Ricci, C.; Hatir, P.C.; Türeli, N.G.; et al. Ciprofloxacin-loaded polymeric nanoparticles incorporated electrospun fibers for drug delivery in tissue engineering applications. *Drug Deliv. Transl. Res.* **2020**, *10*, 706–720, doi:10.1007/s13346-020-00736-1.
8. Catanzano, O.; Acierno, S.; Russo, P.; Cervasio, M.; Del Basso De Caro, M.; Bolognese, A.; Sammartino, G.; Califano, L.; Marenzi, G.; Calignano, A.; et al. Melt-spun bioactive sutures containing nanohybrids for local delivery of anti-inflammatory drugs. *Mater. Sci. Eng. C* **2014**, *43*, 300–309, doi:10.1016/j.msec.2014.07.012.
9. Deng, X.; Qasim, M.; Ali, A. Engineering and polymeric composition of drug-eluting suture: A review. *J. Biomed. Mater. Res. - Part A* **2021**, *109*, 2065–2081, doi:10.1002/jbm.a.37194.
10. Champeau, M.; Thomassin, J.M.; Tassaing, T.; Jérôme, C. Current manufacturing processes of drug-eluting sutures. *Expert Opin. Drug Deliv.* **2017**, *14*, 1293–1303, doi:10.1080/17425247.2017.1289173.
11. Wang, L.; Chen, D.; Sun, J. Layer-by-layer deposition of polymeric microgel films on surgical sutures for loading and release of ibuprofen. *Langmuir* **2009**, *25*, 7990–7994, doi:10.1021/la9004664.
12. Valarezo, E.; Tammaro, L.; Malagón, O.; González, S.; Armijos, C.; Vittoria, V. Fabrication and characterization of poly(lactic acid)/poly(ε-caprolactone) blend electrospun fibers loaded with amoxicillin for tunable delivering. *J. Nanosci. Nanotechnol.* **2015**, *15*, 4706–4712, doi:10.1166/jnn.2015.9726.
13. Li, J.; Pan, H.; Ye, Q.; Shi, C.; Zhang, X.; Pan, W. Carvedilol-loaded polyvinylpyrrolidone electrospun nanofiber film for sublingual delivery. *J. Drug Deliv. Sci. Technol.* **2020**, doi:10.1016/j.jddst.2020.101726.
14. Khan, Z.; Kafiah, F.; Zahid Shafi, H.; Nufaiei, F.; Ahmed Furquan, S.; Matin, A. Morphology, Mechanical Properties and Surface Characteristics of Electrospun Polyacrylonitrile (PAN) Nanofiber Mats. *Int. J. Adv. Eng. Nano Technol.* **2015**.
15. Cirillo, V. Design of Bicomponent Electrospun Conduits for Peripheral Nerve Regeneration.
16. Yan, T.; Shi, Y.; Zhuang, H.; Lin, Y.; Lu, D.; Cao, S.; Zhu, L. Electrospinning mechanism of nanofiber yarn and its multiscale wrapping yarn. *Polymers (Basel).* **2021**, *13*, 1–20, doi:10.3390/polym13183189.
17. Kashiwabuchi, F.; Parikh, K.S.; Omiadze, R.; Zhang, S.; Luo, L.; Patel, H. V; Xu, Q.; Ensign, L.M.; Hanes, J.; Mcdonnell, P.J. Development of Absorbable , Antibiotic-Eluting Sutures for Ophthalmic Surgery. **2017**, *6*, doi:10.1167/tvst.6.1.1.
18. Haghighat, F.; Ravandi, S.A.H. Mechanical properties and in vitro degradation of PLGA suture manufactured via electrospinning. *Fibers Polym.* **2014**, *15*, 71–77, doi:10.1007/s12221-014-0071-9.
19. A.J. Dart; C.M. Dart Biomaterials and Clinical Use. *Sci. Direct* **2011**.
20. He, Y.; Hu, Z.; Ren, M.; Ding, C.; Chen, P.; Gu, Q.; Wu, Q. Evaluation of PHBHHx and PHBV/PLA fibers used as medical sutures. *J. Mater. Sci. Mater. Med.* **2014**, *25*, 561–571, doi:10.1007/s10856-013-5073-4.
21. Shishatskaya, E.I.; Volova, T.G.; Puzyr, A.P.; Mogilnaya, O.A.; Efremov, S.N. Tissue response to the implantation of biodegradable polyhydroxyalkanoate sutures. *J. Mater. Sci. Mater. Med.* **2004**, *15*, 719–728, doi:10.1023/B:JMSM.0000030215.49991.0d.
22. Volova, T.; Shishatskaya, E.; Sevastianov, V.; Efremov, S.; Mogilnaya, O. Results of biomedical investigations of PHB and PHB/PHV fibers. *Biochem. Eng. J.* **2003**, *16*, 125–133, doi:10.1016/S1369-703X(03)00038-X.
23. Melendez-rodriguez, B.; Reis, M.A.M.; Carvalheira, M.; Sammon, C.; Cabedo, L.; Torres-giner, S.; Lagaron, J.M. Development and Characterization of Electrospun Biopapers of Poly (3-hydroxybutyrate- co -3-hydroxyvalerate) Derived from Cheese Whey with Varying 3 - Hydroxyvalerate Contents. **2021**, doi:10.1021/acs.biomac.1c00353.
24. Savenkova, L.; Gercberga, Z.; Bibers, I.; Kalnin, M. Effect of 3-hydroxy valerate content on some physical and mechanical properties of polyhydroxyalkanoates produced by Azotobacter chroococcum. *Process Biochem.* **2000**, *36*, 445–450, doi:10.1016/S0032-9592(00)00235-1.
25. Choudhury, A.; Das, S.; Dhangar, S.; Kapasiya, S.; Kanango, A. Development and characterization buccoadhesive film of ciprofloxacin hydrochloride. *Int. J. PharmTech Res.* **2010**.
26. Melendez-Rodriguez, B.; Castro-Mayorga, J.L.; Reis, M.A.M.; Sammon, C.; Cabedo, L.; Torres-Giner, S.; Lagaron, J.M. Preparation and Characterization of Electrospun Food Biopackaging Films of Poly(3-hydroxybutyrate-co-3-hydroxyvalerate) Derived From Fruit Pulp Biowaste. *Front. Sustain. Food Syst.* **2018**, *2*, 1–16, doi:10.3389/fsufs.2018.00038.

27. Mathematical models of drug release. In *Strategies to Modify the Drug Release from Pharmaceutical Systems*; Elsevier, 2015; pp. 63–86 ISBN 9780081000922.
28. Figueroa-Lopez, K.J.; Andrade-Mahecha, M.M.; Torres-Vargas, O.L. Spice oleoresins containing antimicrobial agents improve the potential use of bio-composite films based on gelatin. *Food Packag. Shelf Life* **2018**, *17*, 50–56, doi:https://doi.org/10.1016/j.fpsl.2018.05.005.
29. Li, H.; Zhang, Z.; Godakanda, V.U.; Chiu, Y.J.; Angkawinitwong, U.; Patel, K.; Stapleton, P.G.; de Silva, R.M.N.; de Silva, K.M.N.; Zhu, L.M.; et al. The effect of collection substrate on electrospun ciprofloxacin-loaded poly(vinylpyrrolidone) and ethyl cellulose nanofibers as potential wound dressing materials. *Mater. Sci. Eng. C* **2019**, *104*, doi:10.1016/j.msec.2019.109917.
30. Okoye, E.; Okolie, T. Development and in vitro characterization of ciprofloxacin loaded polymeric films for wound dressing. *Int. J. Heal. Allied Sci.* **2015**, *4*, 234, doi:10.4103/2278-344x.167660.
31. Sobhani, Z.; Samani, S.M.; Montaseri, H.; Khezri, E. Nanoparticles of chitosan loaded ciprofloxacin: Fabrication and antimicrobial activity. *Adv. Pharm. Bull.* **2017**, *7*, 427–432, doi:10.15171/apb.2017.051.
32. Karimi, K.; Pallagi, E.; Szabó-Révész, P.; Csóka, I.; Ambrus, R. Development of a microparticle-based dry powder inhalation formulation of ciprofloxacin hydrochloride applying the quality by design approach. *Drug Des. Devel. Ther.* **2016**, *10*, 3331–3343, doi:10.2147/DDDT.S116443.
33. Hanafy, A.F. In-vitro bioequivalence, physicochemical and economic benefits study for marketed innovator and generic ciprofloxacin hydrochloride tablets in Saudi Arabia. *J. Appl. Pharm. Sci.* **2016**, *6*, 063–068, doi:10.7324/JAPS.2016.60909.
34. Rovira, F.; Mas, L.C.; Lorena, J.; Mayorga, C. Antimicrobial nanocomposites and electrospun coatings based on poly (3-hydroxybutyrate- co -3-hydroxyvalerate) and copper oxide nanoparticles for active packaging and coating applications. **2018**, *45673*, 1–11, doi:10.1002/app.45673.
35. Pavlova, E.R.; Bagrov, D. V; Kopitsyna, M.N.; Shchelokov, D.A.; Bonartsev, A.P.; Zharkova, I.I.; Mahina, T.K.; Myshkina, V.L.; Bonartseva, G.A.; Shaitan, K. V; et al. Poly (hydroxybutyrate- co -hydroxyvalerate) and bovine serum albumin blend prepared by electrospinning. **2017**, *45090*, 1–9, doi:10.1002/app.45090.
36. Lemes, A.P.; Talim, R.; Gomes, R.C.; Gomes, R.C. Preparation and Characterization of Maleic Anhydride Grafted Poly (Hydroxybutirate-CO-Hydroxyvalerate) – PHBV-g-MA. **2016**, *19*, 229–235.
37. Figueroa-Lopez, K.J.; Torres-Giner, S.; Enescu, D.; Cabedo, L.; Cerqueira, M.A.; Pastrana, L.M.; Lagaron, J.M. Electrospun active biopapers of food waste derived poly(3-hydroxybutyrate-co-3-hydroxyvalerate) with short-term and long-term antimicrobial performance. *Nanomaterials* **2020**, *10*, 506, doi:10.3390/nano10030506.
38. Castro-Mayorga, J.L.; Fabra, M.J.; Lagaron, J.M. Stabilized nanosilver based antimicrobial poly(3-hydroxybutyrate-co-3-hydroxyvalerate) nanocomposites of interest in active food packaging. *Innov. Food Sci. Emerg. Technol.* **2016**, *33*, 524–533, doi:10.1016/j.ifset.2015.10.019.
39. Aytac, Z.; Ipek, S.; Erol, I.; Durgun, E.; Uyar, T. Fast-dissolving electrospun gelatin nanofibers encapsulating ciprofloxacin/cyclodextrin inclusion complex. *Colloids Surfaces B Biointerfaces* **2019**, *178*, 129–136, doi:10.1016/j.colsurfb.2019.02.059.
40. Furukawa, T.; Sato, H.; Murakami, R.; Zhang, J.; Duan, Y.X.; Noda, I.; Ochiai, S.; Ozaki, Y. Structure, dispersibility, and crystallinity of poly(hydroxybutyrate)/ poly(L-lactic acid) blends studied by FT-IR microspectroscopy and differential scanning calorimetry. *Macromolecules* **2005**, *38*, 6445–6454, doi:10.1021/ma0504668.
41. Wu, Q.; Li, Z.; Hong, H.; Yin, K.; Tie, L. Adsorption and intercalation of ciprofloxacin on montmorillonite. *Appl. Clay Sci.* **2010**, *50*, 204–211, doi:10.1016/j.clay.2010.08.001.
42. Li, H.; Williams, G.R.; Wu, J.; Wang, H.; Sun, X.; Zhu, L.M. Poly(N-isopropylacrylamide)/poly(L-lactic acid-co-ε-caprolactone) fibers loaded with ciprofloxacin as wound dressing materials. *Mater. Sci. Eng. C* **2017**, *79*, 245–254, doi:10.1016/j.msec.2017.04.058.
43. Nunes, S.P.; Culfaz-Emecen, P.Z.; Ramon, G.Z.; Visser, T.; Koops, G.H.; Jin, W.; Ulbricht, M. Thinking the future of membranes: Perspectives for advanced and new membrane materials and manufacturing processes. *J. Memb. Sci.* **2020**, *598*, 117761, doi:10.1016/j.memsci.2019.117761.
44. Teno, J.; Pardo-Figuerez, M.; Figueroa-Lopez, K.J.; Prieto, C.; Lagaron, J.M. Development of Multilayer Ciprofloxacin Hydrochloride Electrospun Patches for Buccal Drug Delivery. *J. Funct. Biomater.* **2022**, *13*, 170, doi:10.3390/jfb13040170.
45. Liu, S.; Yu, J.; Li, H.; Wang, K.; Wu, G.; Li, F.; Zhang, M. Controllable Drug Release Behavior of Polylactic Acid (PLA) Surgical Suture Coating with. *Polymers (Basel).* **2020**, *12*.
46. Kamal, R.; Razzaq, A.; Ali shah, K.; Khan, Z.U.; Khan, N.U.; Menaa, F.; Iqbal, H.; Cui, J. Evaluation of cephalexin-loaded PHBV nanofibers for MRSA-infected diabetic foot ulcers treatment. *J. Drug Deliv. Sci. Technol.* **2022**, *71*, 103349, doi:10.1016/j.jddst.2022.103349.
47. Wei, L.; Wu, S.; Shi, W.; Aldrich, A.L.; Kielian, T.; Carlson, M.A.; Sun, R.; Qin, X.; Duan, B. Large-Scale and

Rapid Preparation of Nanofibrous Meshes and Their Application for Drug-Loaded Multilayer Mucoadhesive Patch Fabrication for Mouth Ulcer Treatment. *ACS Appl. Mater. Interfaces* **2019**, *11*, 28740–28751, doi:10.1021/acsami.9b10379.

48. Odermatt, E.K.; Funk, L.; Bargon, R.; Martin, D.P.; Rizk, S.; Williams, S.F. MonoMax suture: A new long-term absorbable monofilament suture made from poly-4-hydroxybutyrate. *Int. J. Polym. Sci.* **2012**, *2012*, doi:10.1155/2012/216137.
49. Williams, S.F.; Rizk, S.; Martin, D.P. Poly-4-hydroxybutyrate (P4HB): A new generation of resorbable medical devices for tissue repair and regeneration. *Biomed. Tech.* **2013**, *58*, 439–452, doi:10.1515/bmt-2013-0009.
50. Albertsmeier, M.; Seiler, C.M.; Fischer, L.; Baumann, P.; Hüsing, J.; Seidlmayer, C.; Franck, A.; Jauch, K.W.; Knaebel, H.P.; Büchler, M.W. Evaluation of the safety and efficacy of MonoMax® suture material for abdominal wall closure after primary midline laparotomy - A controlled prospective multicentre trial: ISSAAC [NCT005725079]. *Langenbeck's Arch. Surg.* **2012**, *397*, 363–371, doi:10.1007/s00423-011-0884-6.
51. Zhao, H.; Cui, Z.; Sun, X.; Turng, L.S.; Peng, X. Morphology and properties of injection molded solid and microcellular polylactic acid/polyhydroxybutyrate-valerate (PLA/PHBV) blends. *Ind. Eng. Chem. Res.* **2013**, *52*, 2569–2581, doi:10.1021/ie301573y.
52. Padmakumar, S.; Joseph, J.; Neppalli, M.H.; Mathew, S.E.; Nair, S. V.; Shankarappa, S.A.; Menon, D. Electrospun Polymeric Core-sheath Yarns as Drug Eluting Surgical Sutures. *ACS Appl. Mater. Interfaces* **2016**, *8*, 6925–6934, doi:10.1021/acsami.6b00874.